Electronic Supplementary Material (ESI) for Chemical Communications

Electronic Supplementary Information (ESI)

Novel Bipolar AIE-active Luminogens Comprised of an Oxadiazole Core and Terminal TPE Moieties as New Type of Host for Doped Electroluminescence

Jing Huang,[a] Xiao Yang,[b] Xianjie Li,[c] Pengyu Chen,[a] Runli Tang,[a] Ping Lu,[c] Yuguang Ma,[c] Lei Wang,*[b] Jingui Qin,[a] and Zhen Li*[a]

[a] Department of Chemistry, Hubei Key Lab on Organic and Polymeric Opto-Electronic Materials, Wuhan University, Wuhan 430072, China.
E-mail: lizhen@whu.edu.cn
[b] Wuhan National Laboratory for Optoelectronics, School of Optoelectronic Science and Engineering, Huazhong University of Science and Technology, Wuhan 430074, China
E-mail: lei96wang@163.com.
[c] State Key Laboratory of Supramolecular Structure and Materials, Department of Chemistry, Jilin University, Jilin 130022, China.

Experimental Section

Characterization

^{1}H and ^{13}C NMR spectra were measured on a Mecuryvx300 spectrometer. Elemental analyses of carbon, hydrogen, and nitrogen were performed on a CARLOERBA-1106 microanalyzer. Mass spectra were measured on a ZAB 3F-HF mass spectrophotometer. UV-vis absorption spectra were recorded on a Shimadzu UV-2500 recording spectrophotometer. Photoluminescence spectra were recorded on a Hitachi F-4500 fluorescence spectrophotometer. Differential scanning calorimetry (DSC) was performed on a NETZSCH DSC 200 PC unit at a heating rate of 15 ^{o}C min^{-1} from room temperature to 300 ^{o}C under argon. The glass transition temperature (T_g) was determined from the second heating scan. Thermogravimetric analysis (TGA) was undertaken with a NETZSCH STA 449C instrument. The thermal stability of the samples under a nitrogen atmosphere was determined by measuring their weight loss while heating at a rate of 10 ^{o}C/min from 25 to 600 ^{o}C. Cyclic voltammetry (CV) was carried out on a CHI voltammetric analyzer in a three-electrode cell with a Pt counter electrode, a Ag/AgCl reference electrode, and a glassy carbon working electrode at a scan rate of 100 mVs^{-1} with 0.1 M tetrabutylammonium perchlorate (purchased from Alfa Aesar) as the supporting electrolyte, in anhydrous dichloromethane solution purged with nitrogen. The potential values obtained in reference to the Ag/Ag^{+} electrode were converted to values versus the saturated calomel electrode (SCE) by means of an internal ferrocenium/ferrocene (Fc^{+}/Fc) standard.

Computational details

The geometrical and electronic properties were optimized at B3LYP/6-31g(d) level using Gaussian 09 program. The molecular orbitals were obtained at the same level of theory.

TOF Measurement

Time-of-flight (TOF) transient photocurrent technique was used to measure the carriers' mobility using a simple device configuration of ITO/Oxa-*p*TPE and Oxa-*m*TPE (5.9 or 4 μm)/Alq3(50 nm)/Al(100 nm), and Alq3 is used as a charge-generation layer. Samples, Alq_3 and Al were sequentially deposited onto the ITO substrate in the vacuum of 10^{-5} Torr. A Nd:YAG (λ=355 nm, pulse: 5 ns) was used at the light source for the photo-generating charge carriers. For the electron-mobility measurement, the charge carriers were generated at the Alq3 layer when a positive voltage was applied. Then the electron moved toward the ITO contact, and the corresponding displacement current was measured across the load resistor using a digital storage oscilloscope (DPO7104; bandwidth: 1GHz). In contrast, the hole mobility could be obtained by negatively biasing to the Al contact. The carriers' mobilities were calculated from the transition time t_T via the equation $\mu = d^2/Vt_T$, where d was the thickness of the sample layer and V was the applied voltage.

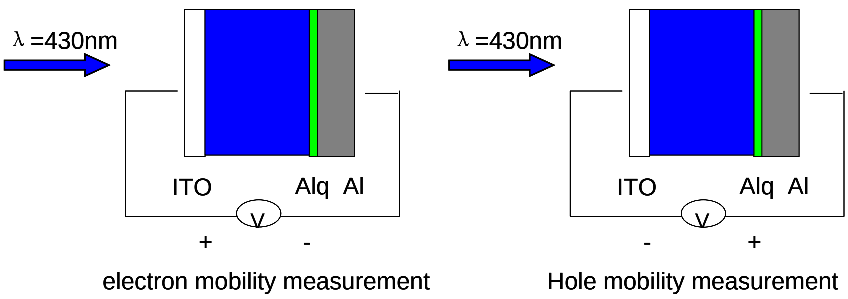

OLED device fabrication and measurement

The hole-transporting material NPB (1,4-bis(1-naphthylphenylamino)-biphenyl), electron-transporting materials 1,3,5-tris(N-phenylbenzimidazol-2-yl)benzene (TPBI) and tris(8-hydroxyquinolinato)aluminium (Alq_3) were purchased from Changzhou Mascot Import & Export Co., LTD. The EL devices were fabricated by vacuum deposition of the materials at a base pressure of 5×10^{-6} Torr onto glass precoated with a layer of indium tin oxide (ITO) with a sheet resistance of 25 Ω/square. Before the deposition of an organic layer, the clear ITO substrates were treated with oxgen plasma for 3 min. The deposition rate of organic compounds was 0.9-1.1 Å s^{-1}. Finally, a cathode composed of lithium fluoride (1 nm) and aluminium (100 nm) was sequentially deposited onto the substrate in the vacuum of 10^{-5} Torr. The *L–V–J* of the devices was measured with a Keithley 2400 Source meter and PR655. The EL spectra were measured by PR655. All measurements were carried out at room temperature under ambient conditions.

Preparation of compounds

All other chemicals and reagents were obtained from commercial sources and used as received without further purification. Solvents for chemical synthesis were purified according to the standard procedures. 3-Bromobenzophenone,[1] *p*-TPE-Br, compound **2** and **3** were synthesized according to the literatures.

Synthesis of *m*TPE-Br

A 2.3 M solution of *n*-butyllithium in hexane (4.09 mmol, 1.78 mL) was added to a solution of diphenylmethane (0.86 g, 5.12 mmol) in anhydrous tetrahydrofuran (40 mL) at 0 °C under an argon atmosphere. After stirring for 1 h at this temperature, 3- bromobenzophenone (0.89 g, 3.41 mmol) was added. After 2 h, the mixture was slowly warmed to room temperature. Then, the reaction was quenched with an aqueous solution of ammonium chloride and the mixture was extracted with dichloromethane. The organic layer was evaporated after drying with anhydrous sodium sulfate and the resulting crude product was dissolved in toluene (25 mL). The *p*-toluenesulfonic acid (0.12 g, 0.68 mmol) was added, and the mixture was refluxed overnight and cooled to room temperature. The mixture was evaporated and the crude product was purified by silica gel column chromatography using petroleum ether as eluent to obtain a white powder in the yield of 50% (0.7 g). ^{1}H NMR (300 MHz, $CDCl_3$, δ): 7.20-7.11 (m, 11H), 7.02-7.01 (m, 5H), 6.96-6.95 (m, 2H); ^{13}C NMR (75 MHz, $CDCl_3$, δ): 146.0, 143.4, 143.3, 143.1, 142.2, 139.5, 134.2, 131.3, 130.1, 129.6, 129.3, 128.0, 127.8, 126.9, 126.8, 121.9; MS (EI), m/z: 412.13 ([M^+], calcd for $C_{26}H_{19}Br$, 411.33).

Synthesis of Compound 1

A 2.3 M solution of *n*-butyllithium in hexane (15.0 mmol, 6.5mL) was added to a solution of *m*-TPE-Br (4.12 g, 10.0 mmol) in anhydrous tetrahydrofuran (60 mL) at -78 ^{o}C under an argon atmosphere. After stirring for 4 h, 2-isopropoxy-4, 4,5,5-tetramethyl-1,3,2-dioxaborolane (6.1 mL) was added. After 2 h, the mixture was slowly warmed to room temperature. After stirring overnight, the reaction was terminated by the added brine. The mixture was extracted with dichloromethane and the organic layer was combined, and dried with anhydrous sodium sulfate. After filtration and solvent evaporation, the crude product was purified by silica gel column chromatography using petroleum ether/dichloromethane (v/v=5/1) as eluent. White powder of **1** was obtained in the yield of 60% (2.30 g). ^{1}H NMR (300 MHz, $CDCl_3$, δ): 7.53-7.48 (m, 2H), 7.09-7.02 (m, 17H), 1.28 (s, 12H); ^{13}C NMR (75 MHz, $CDCl_3$, δ): 143.6, 143.3, 142.9, 141.1, 140.8, 137.5, 134.2, 132.7, 131.3, 131.2, 127.5, 127.0, 126.3, 126.2, 83.6, 24.7; MS (EI), m/z: 458.35 ([M^+], calcd for $C_{32}H_{31}BO_2$, 458.40).

Synthesis of Oxa-*m*TPE

A mixture of compound **3** (380 mg, 1 mmol), compound **1** (940 mg, 2.05 mmol), $Pd(PPh_3)_4$ (0.10 g, 4% mmol) and potassium hydroxide (560 mg, 10 mmol) in 15 mL of THF and 3 mL of distilled water in a 50 ml Schlenk tube was refluxed for 2 days under argon. The mixture was extracted with dichloromethane. The combined organic extracts were dried over anhydrous Na_2SO_4 and concentrated by rotary evaporation. The crude product was purified by column chromatography on silica gel using dichloromethane/petroleum ether (v/v=1/1) as eluent to afford the product as a white powder in the yield of 63.2% (758 mg). ^{1}H NMR (300 MHz, $CDCl_3$, δ): 7.55-7.52 (m, 2H), 7.42-7.33 (m, 4H), 7.09-7.02 (m, 35H), 6.91-6.90 (m, 5H); ^{13}C NMR (75 MHz, $CDCl_3$, δ): 164.5, 143.8, 143.7, 143.6, 143.3, 142.1, 141.4, 140.6, 139.9, 132.0, 131.5, 131.4, 131.3, 131.2, 130.9, 130.4, 129.7, 127.8, 127.7, 127.4, 127.1, 126.5, 122.6; MS (EI), m/z: 882.28 ([M+], calcd for $C_{66}H_{46}N_2O$, 883.08); Anal. Calcd for $C_{66}H_{46}N_2O$: C, 89.77; H, 5.25; N, 3.17. Found: C, 89.55; H, 4.94; N, 3.44.

Synthesis of Oxa-*p*TPE

The synthetic procedure was similar to that of **Oxa-*m*TPE**, with compound **2** and **1** as the starting materials. White solid. Yield: 68%. ^{1}H NMR (300 MHz, $CDCl_3$, δ): 7.78-7.76 (m, 2H), 7.59-7.40 (m, 6H), 7.08-6.97 (m, 26H), 6.93-6.88 (m, 12H); ^{13}C NMR (75 MHz, $CDCl_3$, δ): 165.3, 144.0, 143.8, 143.7, 143.1, 142.3, 141.5, 140.5, 138.5, 131.6, 131.4, 131.3, 130.5, 128.3, 127.9, 127.8, 127.7, 126.8, 126.6, 123.0; MS (EI), m/z: 882.94 ([M+], calcd for $C_{66}H_{46}N_2O$, 883.08); Anal. Calcd for $C_{66}H_{46}N_2O$: C, 89.77; H, 5.25; N, 3.17. Found: C, 89.62; H, 5.23; N, 3.44.

_(1) Tobias J. Korn and P. Knochel, *Angew. Chem., Int. Ed.* 2001, **40**, 74.

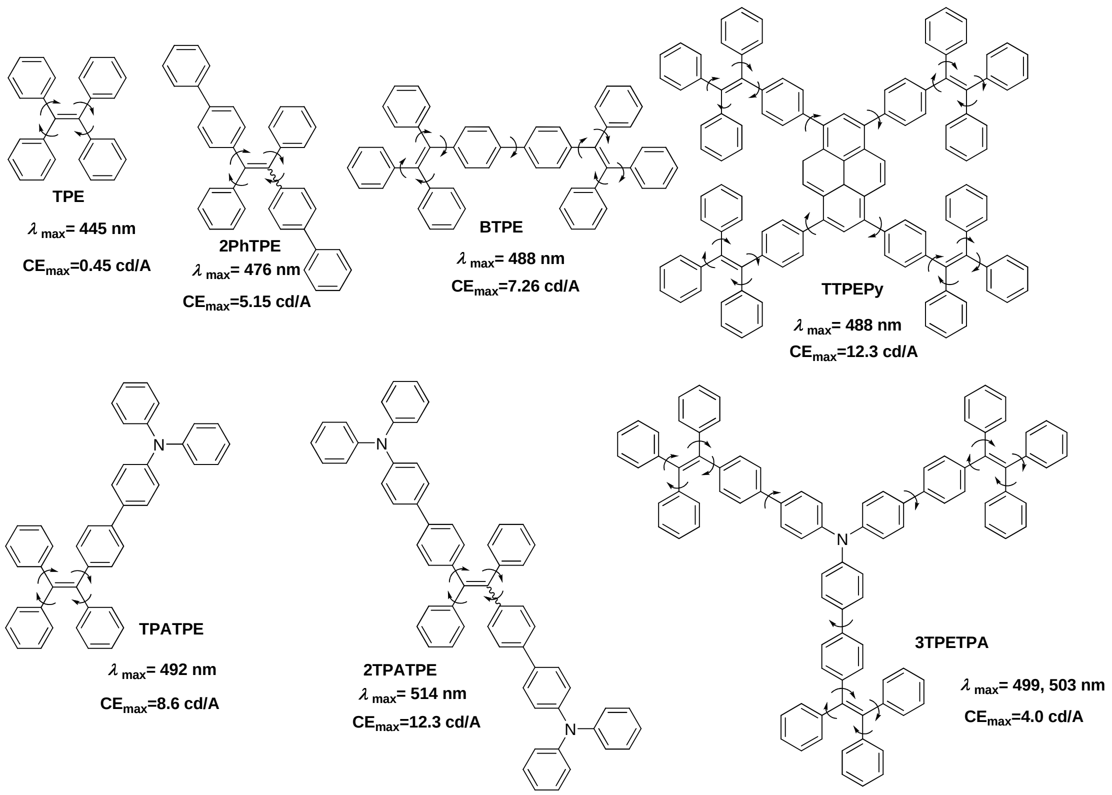

Chart S1. The EL peaks and maximum current efficiencies of TPE and typical TPE-based luminogens.

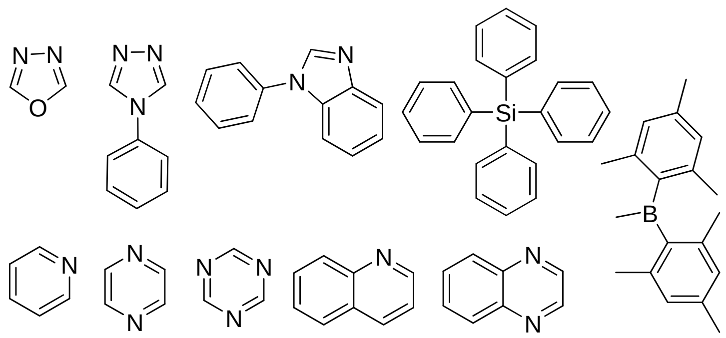

Chart S2. Representative electron-transporting moieties.

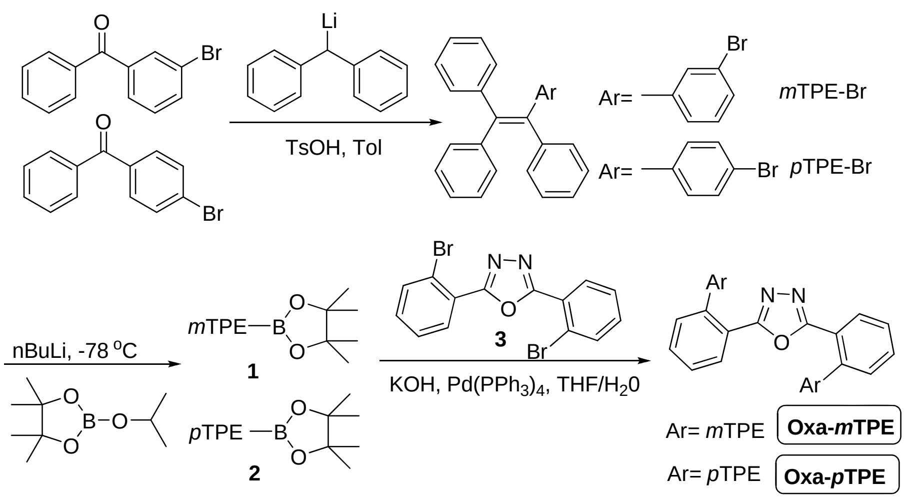

Scheme S1. Synthetic routes to Oxa-*m*TPE and Oxa-*p*TPE.

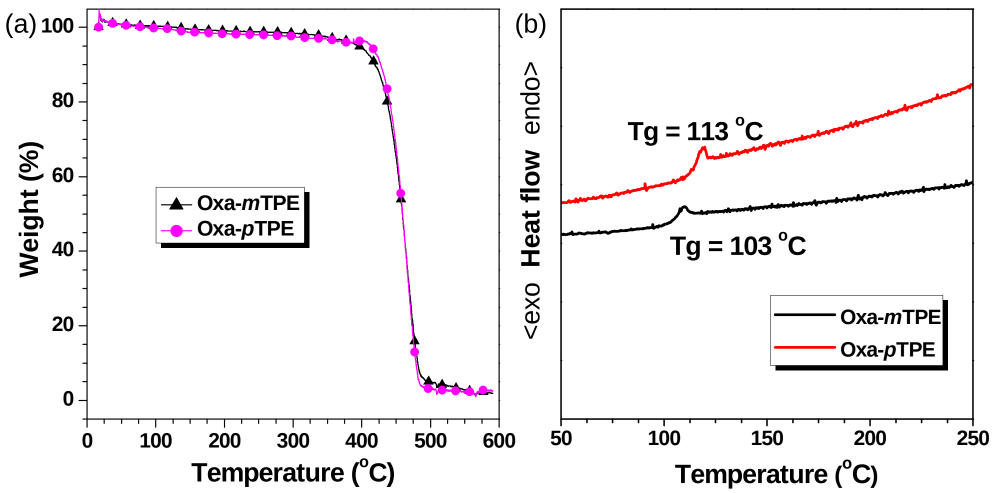

Figure S1. (a) TGA and (b) DSC (second heating cycle) thermograms of **Oxa-*m*TPE** and **Oxa-*p*TPE** recorded under N_2 at a heating rate of (A) 10 and (B)15 °C/min.

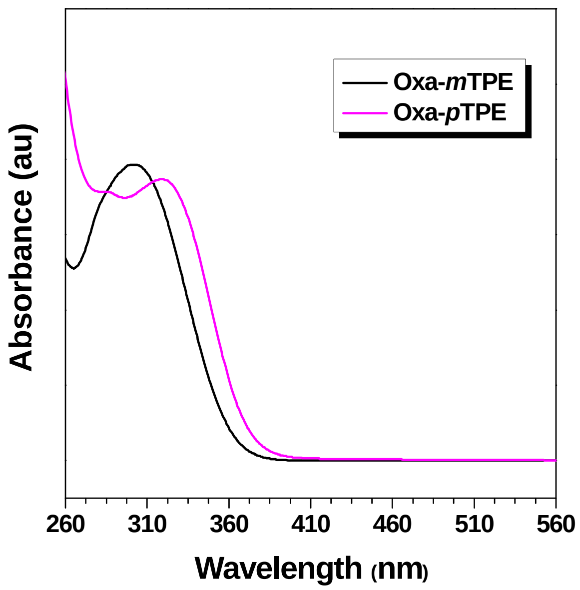

Figure S2. UV spectra in THF solution. Concentration (μM): 12.1 and 10.7 for **Oxa-*m*TPE** and **Oxa-*p*TPE**, respectively.

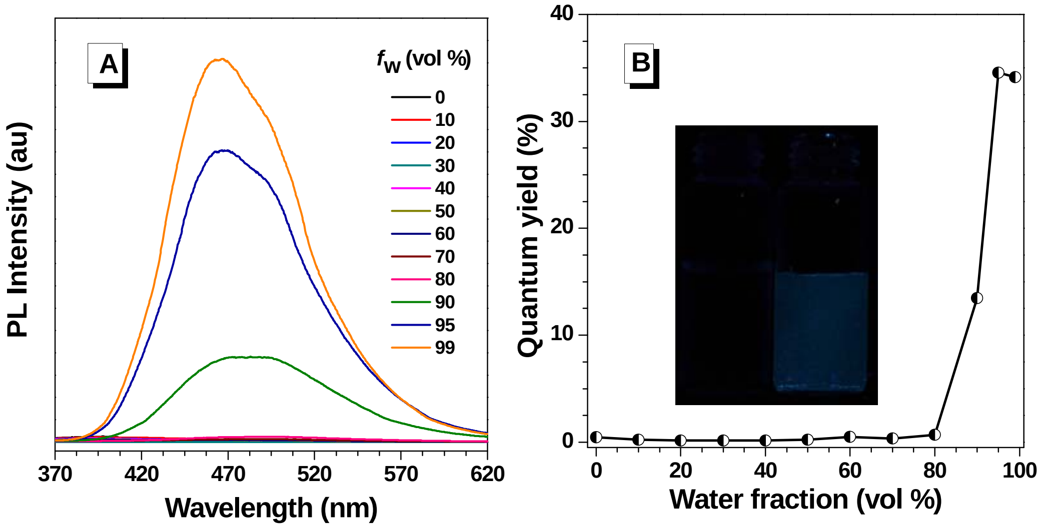

Figure S3. (A) PL spectra of **Oxa-*m*TPE** in THF/H_2O mixtures with different water fractions (f_w). Concentration (μM): 12.1; excitation wavelength (nm): 320. (B) Plots of fluorescence quantum yields determined in THF/H_2O solutions using 9,10-diphenylanthracene (Φ = 90% in cyclohexane) as standard versus water fractions. Inset in (B): photos of **Oxa-*m*TPE** in THF/water mixtures (f_w=0 and 99%) taken under the illumination of a 365 nm UV lamp.

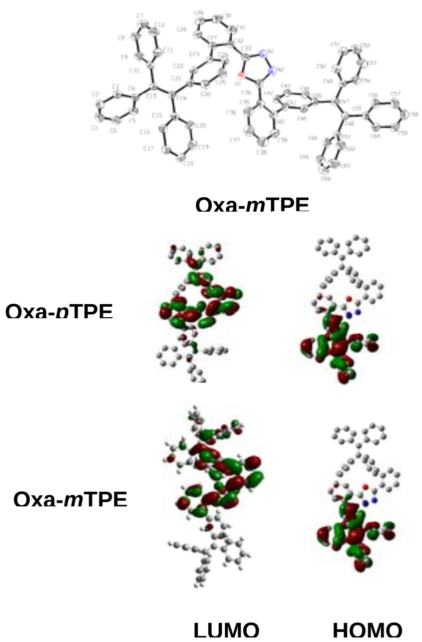

Figure S4. ORTEP drawing of **Oxa-*m*TPE** and calculated molecular orbital amplitude plots of HOMO and LUMO levels of **Oxa-*p*TPE** and **Oxa-*m*TPE**.

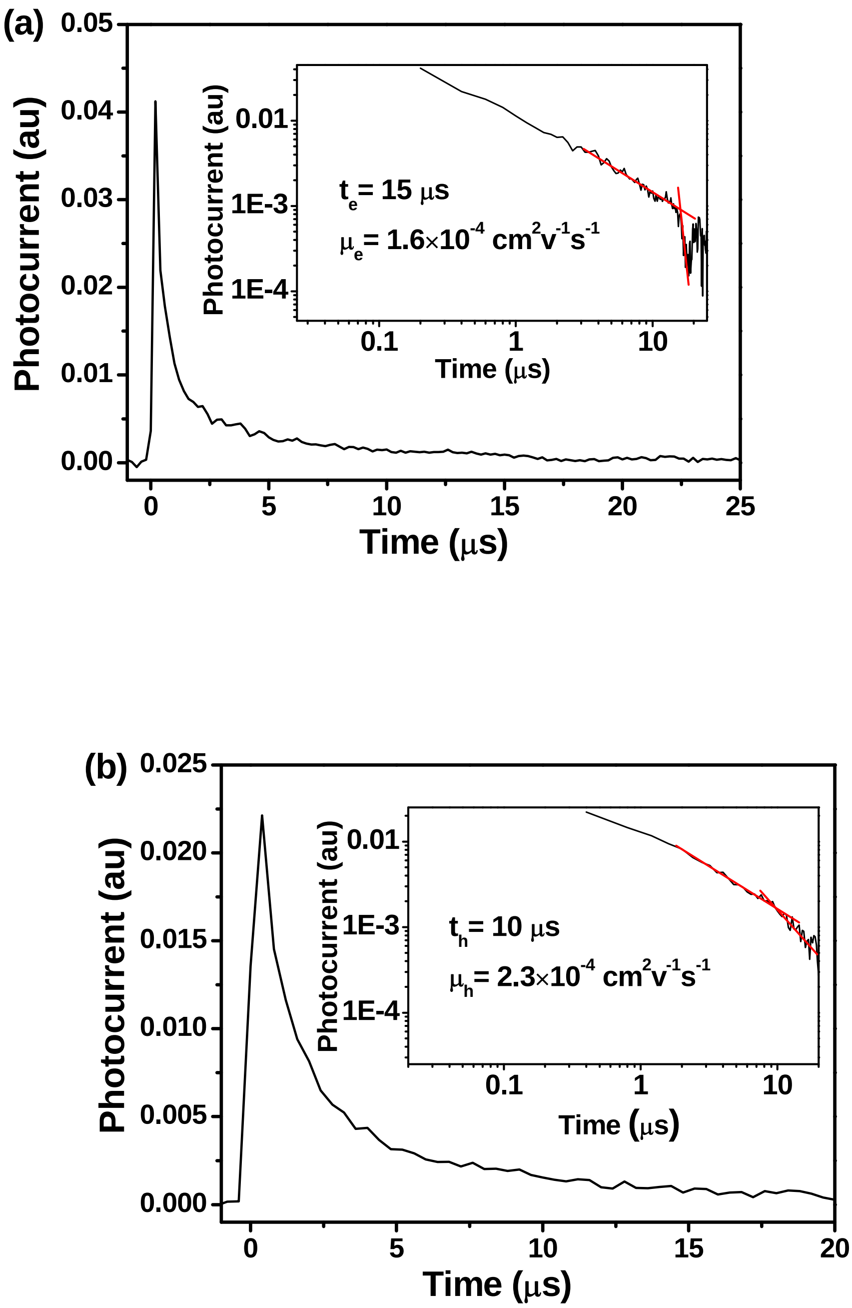

Figure S5. Representative TOF transients for **Oxa-*p*TPE** (5.9 μm thick): (a) electron and (b) hole at an electric field $E = 2.5\times10^{-5}$ Vcm^{-1}. Insets of (a) and (b) are double logarithmic plots of (a) and (b), respectively.

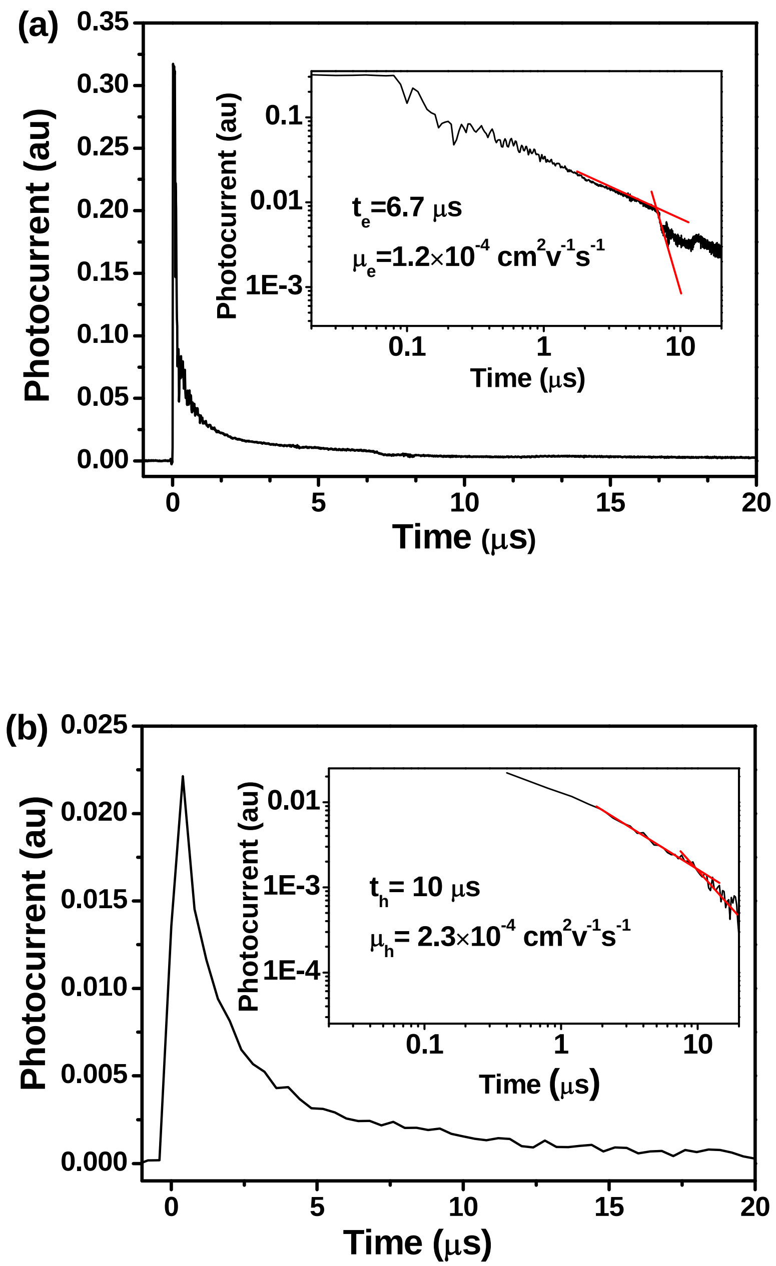

Figure S6. Representative TOF transients for **Oxa-*m*TPE** (4 μm thick): (a) electron and (b) hole at an electric field $E = 5\times10^{-5}$ Vcm^{-1}. Insets of (a) and (b) are double logarithmic plots of (a) and (b), respectively.

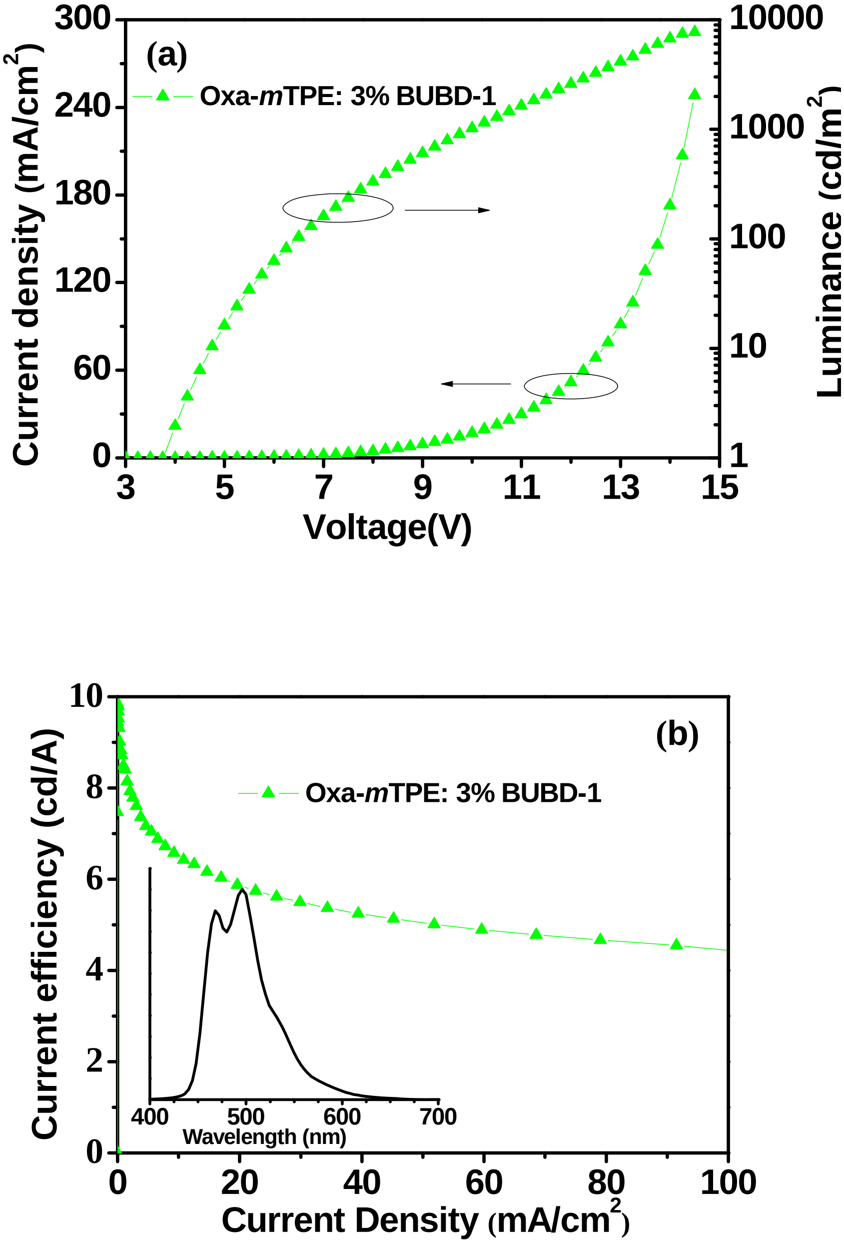

Figure S7. Changes in a) current density and luminance with the applied voltage and b) current efficiency with the current density in BUBD-1 doped multilayer EL devices of **Oxa-*m*TPE**. Inset in panel (b): EL spectrum of the device. Device configuration: ITO/NPB(20 nm)/ Oxa-*m*TPE: 3% BUBD-1(40nm)/TPBi(10nm)/Alq3(20nm)/Al(100nm).

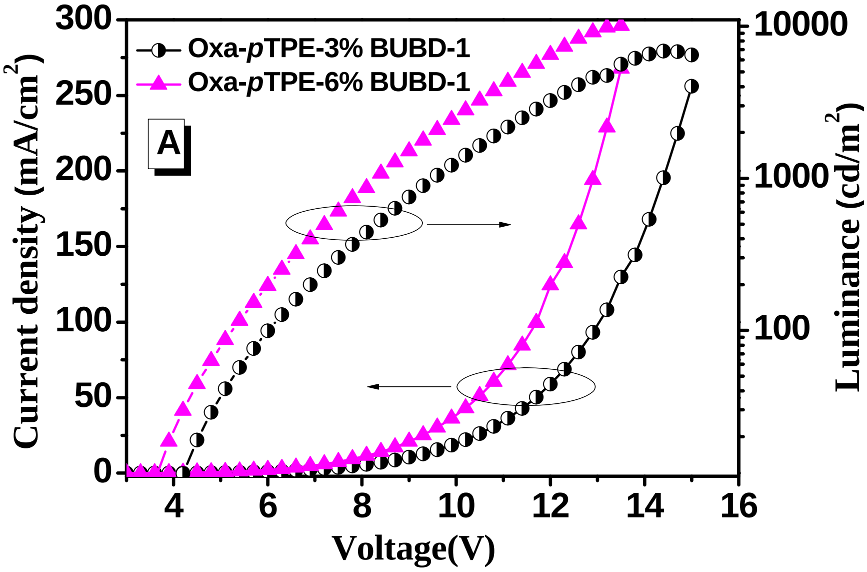

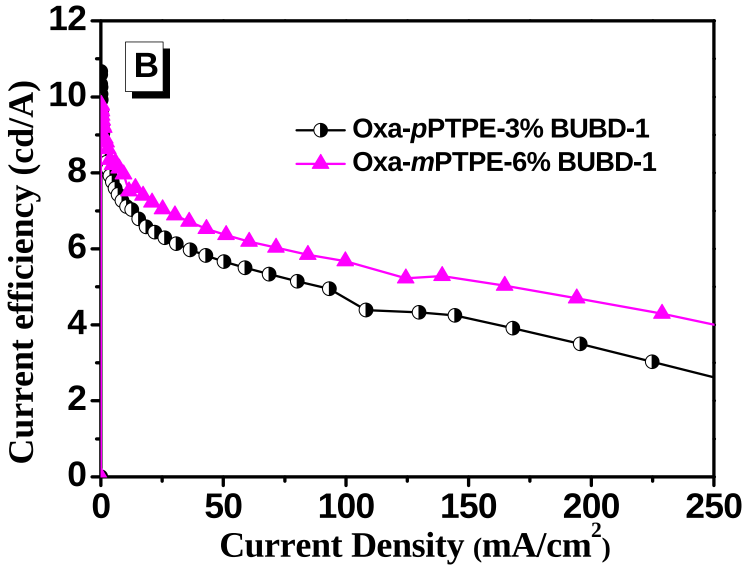

Figure S8. Changes in (A) current density and luminance with the applied voltage and (B) current efficiency with the current density in BUBD-1 doped multilayer EL devices of **Oxa-*p*TPE** with different doping concentration.

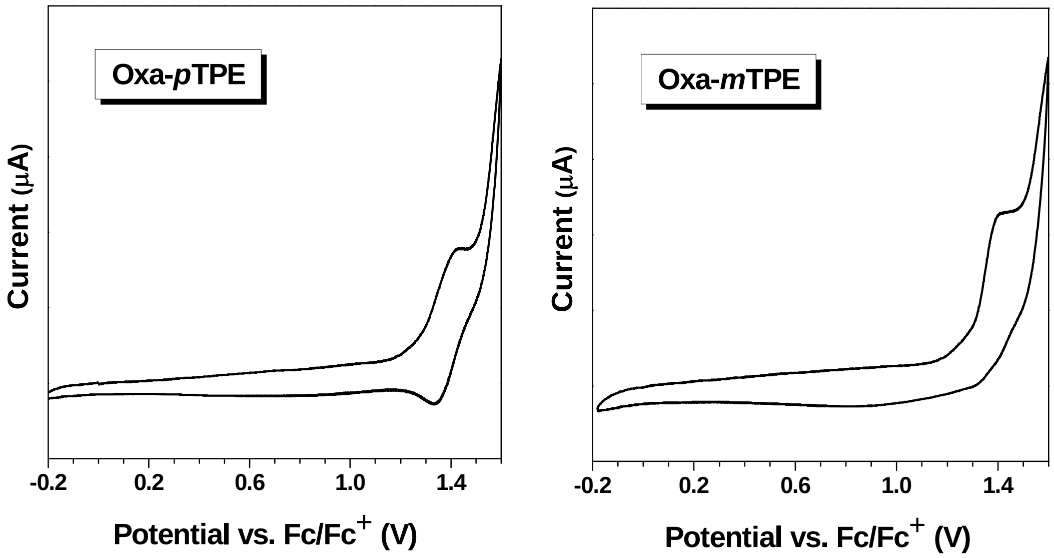

Figure S9. Cyclic Voltammograms of **Oxa-*p*TPE** and **Oxa-*m*TPE** in CH_2Cl_2.

Table S1. The thermal, electrochemical and photophysical data of **Oxa-*p*TPE** and **Oxa-*m*TPE**.

	$T_d{}^a$ (°C)	T_g (°C)	$E_g{}^b$ (eV)	$E_{HOMO}{}^c$ (eV)	$E_{LUMO}{}^d$ (eV)	$\lambda_{abs}{}^e$ (nm)	PL λ_{max} (aggr)^f (nm)	PL λ_{max} (film) (nm)
Oxa-*p*TPE	414	113	3.30	5.55	2.25	320	479	480
Oxa-*m*TPE	400	103	3.39	5.57	2.18	302	465	464

[a] 5% weight loss temperature measured by TGA under N_2. [b] Band gap estimated from optical absorption band edge of the solution. [c] Calculated from the onset oxidation potentials of the polymers. [d] Estimated using empirical equations $E_{LUMO}=E_{HOMO}+E_g$. [e] Observed from absorption spectra in dilute THF solution. [f] Determined in THF:H_2O=1:99 solution.

Table S2. EL performances of **Oxa-*p*TPE** and **Oxa-*m*TPE**.[a]

	V_{on} (V)	L_{max} (cd m^{-2})	$\eta_{P, max}$ (Im w^{-1})	$\eta_{C, max}$ (cd A^{-1})	$\eta_{ext, max}$ (%)	CIE (x,y)
Oxa-*p*TPE	5.10	10070	9.92	9.79	4.73	0.15, 0.34
Oxa-*m*TPE	6.25	7734	7.96	9.82	5.0	0.15, 0.33

[a] Abbreviations: V_{on} = turn-on voltage at 1 cd m^{-2}, L_{max} = maximum luminance, $\eta_{C, max}$, $\eta_{C, max}$ and $\eta_{ext, max}$ = maximum power, current and external efficiencies, respectively. CIE= Commission International de l'Eclairage coordinates.

Table S3. Bond lengths [Å] and angles [°] for **Oxa-*m*TPE**.

C(1)-C(6)	1.365(8)
C(1)-C(2)	1.366(8)
N(1)-C(33)	1.276(5)
N(1)-N(2)	1.394(6)
O(1)-C(33)	1.372(4)
O(1)-C(34)	1.361(5)
C(2)-C(3)	1.375(6)
N(2)-C(34)	1.294(5)
C(3)-C(4)	1.398(6)
C(4)-C(5)	1.385(6)
C(4)-C(13)	1.486(5)
C(5)-C(6)	1.377(6)
C(7)-C(8)	1.364(7)
C(7)-C(12)	1.378(7)
C(8)-C(9)	1.368(6)
C(9)-C(10)	1.385(6)
C(10)-C(11)	1.383(6)
C(10)-C(13)	1.496(5)
C(11)-C(12)	1.388(6)
C(13)-C(14)	1.357(5)
C(14)-C(21)	1.488(5)
C(14)-C(15)	1.496(5)
C(15)-C(16)	1.383(5)
C(15)-C(20)	1.392(6)
C(16)-C(17)	1.376(5)
C(17)-C(18)	1.372(6)
C(18)-C(19)	1.373(6)
C(19)-C(20)	1.371(6)
C(21)-C(22)	1.388(5)
C(21)-C(26)	1.383(6)
C(22)-C(23)	1.387(5)
C(23)-C(24)	1.382(5)
C(23)-C(27)	1.487(5)
C(24)-C(25)	1.377(6)
C(25)-C(26)	1.393(6)
C(27)-C(28)	1.388(5)
C(27)-C(32)	1.416(5)
C(28)-C(29)	1.375(6)
C(29)-C(30)	1.363(7)
C(30)-C(31)	1.378(7)
C(31)-C(32)	1.400(6)
C(32)-C(33)	1.466(6)
C(34)-C(35)	1.462(6)
C(35)-C(40)	1.396(6)
C(35)-C(36)	1.390(6)

C(36)-C(37)	1.354(7)
C(37)-C(38)	1.386(8)
C(38)-C(39)	1.376(7)
C(39)-C(40)	1.410(6)
C(40)-C(41)	1.478(6)
C(41)-C(42)	1.389(6)
C(41)-C(46)	1.397(5)
C(42)-C(43)	1.370(6)
C(43)-C(44)	1.379(6)
C(44)-C(45)	1.377(6)
C(45)-C(46)	1.393(6)
C(45)-C(47)	1.505(6)
C(47)-C(48)	1.321(5)
C(47)-C(49)	1.490(6)
C(48)-C(55)	1.500(6)
C(48)-C(61)	1.508(6)
C(49)-C(50)	1.382(6)
C(49)-C(54)	1.397(6)
C(50)-C(51)	1.393(7)
C(51)-C(52)	1.366(8)
C(52)-C(53)	1.342(8)
C(53)-C(54)	1.369(7)
C(55)-C(56)	1.380(6)
C(55)-C(60)	1.384(6)
C(56)-C(57)	1.366(7)
C(57)-C(58)	1.356(8)
C(58)-C(59)	1.355(8)
C(59)-C(60)	1.395(7)
C(61)-C(62)	1.381(7)
C(61)-C(66)	1.379(6)
C(62)-C(63)	1.394(7)
C(63)-C(64)	1.381(10)
C(64)-C(65)	1.337(9)
C(65)-C(66)	1.369(7)

C(6)-C(1)-C(2)	119.6(5)
C(33)-N(1)-N(2)	106.6(4)
C(33)-O(1)-C(34)	102.7(3)
C(1)-C(2)-C(3)	120.3(5)
C(34)-N(2)-N(1)	106.9(4)
C(4)-C(3)-C(2)	121.0(5)
C(3)-C(4)-C(5)	117.5(4)
C(3)-C(4)-C(13)	119.7(4)
C(5)-C(4)-C(13)	122.7(4)
C(6)-C(5)-C(4)	120.7(5)
C(1)-C(6)-C(5)	120.9(5)
C(8)-C(7)-C(12)	119.9(4)
C(7)-C(8)-C(9)	119.8(5)

C(10)-C(9)-C(8)	122.0(4)
C(9)-C(10)-C(11)	117.6(4)
C(9)-C(10)-C(13)	120.4(4)
C(11)-C(10)-C(13)	121.9(4)
C(10)-C(11)-C(12)	120.6(4)
C(7)-C(12)-C(11)	120.0(5)
C(14)-C(13)-C(10)	122.3(3)
C(14)-C(13)-C(4)	123.9(3)
C(10)-C(13)-C(4)	113.8(3)
C(13)-C(14)-C(21)	121.9(3)
C(13)-C(14)-C(15)	122.5(3)
C(21)-C(14)-C(15)	115.5(3)
C(16)-C(15)-C(20)	117.3(4)
C(16)-C(15)-C(14)	123.0(3)
C(20)-C(15)-C(14)	119.8(3)
C(15)-C(16)-C(17)	120.9(4)
C(18)-C(17)-C(16)	121.1(4)
C(19)-C(18)-C(17)	118.5(4)
C(18)-C(19)-C(20)	120.8(4)
C(15)-C(20)-C(19)	121.2(4)
C(22)-C(21)-C(26)	118.2(4)
C(22)-C(21)-C(14)	120.3(4)
C(26)-C(21)-C(14)	121.6(3)
C(21)-C(22)-C(23)	122.1(4)
C(24)-C(23)-C(22)	118.3(3)
C(24)-C(23)-C(27)	120.8(3)
C(22)-C(23)-C(27)	120.8(3)
C(23)-C(24)-C(25)	121.0(4)
C(24)-C(25)-C(26)	119.8(4)
C(21)-C(26)-C(25)	120.6(4)
C(28)-C(27)-C(32)	117.6(4)
C(28)-C(27)-C(23)	120.3(3)
C(32)-C(27)-C(23)	122.0(3)
C(27)-C(28)-C(29)	121.8(4)
C(30)-C(29)-C(28)	120.3(4)
C(29)-C(30)-C(31)	120.2(4)
C(30)-C(31)-C(32)	120.3(4)
C(31)-C(32)-C(27)	119.6(4)
C(31)-C(32)-C(33)	118.8(4)
C(27)-C(32)-C(33)	121.5(4)
N(1)-C(33)-O(1)	112.2(4)
N(1)-C(33)-C(32)	129.8(4)
O(1)-C(33)-C(32)	117.9(3)
N(2)-C(34)-O(1)	111.5(4)
N(2)-C(34)-C(35)	130.8(4)
O(1)-C(34)-C(35)	117.7(4)
C(40)-C(35)-C(36)	120.6(4)
C(40)-C(35)-C(34)	121.2(4)

C(36)-C(35)-C(34)	118.2(4)
C(37)-C(36)-C(35)	120.8(5)
C(36)-C(37)-C(38)	120.3(5)
C(39)-C(38)-C(37)	119.8(5)
C(38)-C(39)-C(40)	121.1(5)
C(35)-C(40)-C(39)	117.4(4)
C(35)-C(40)-C(41)	123.1(4)
C(39)-C(40)-C(41)	119.4(4)
C(42)-C(41)-C(46)	118.4(4)
C(42)-C(41)-C(40)	120.5(4)
C(46)-C(41)-C(40)	121.1(4)
C(43)-C(42)-C(41)	120.6(4)
C(42)-C(43)-C(44)	120.4(4)
C(45)-C(44)-C(43)	120.8(4)
C(44)-C(45)-C(46)	118.6(4)
C(44)-C(45)-C(47)	119.6(4)
C(46)-C(45)-C(47)	121.6(4)
C(41)-C(46)-C(45)	121.2(4)
C(48)-C(47)-C(49)	123.2(4)
C(48)-C(47)-C(45)	122.3(4)
C(49)-C(47)-C(45)	114.4(3)
C(47)-C(48)-C(55)	122.8(4)
C(47)-C(48)-C(61)	122.8(4)
C(55)-C(48)-C(61)	114.4(3)
C(50)-C(49)-C(54)	117.1(4)
C(50)-C(49)-C(47)	119.4(4)
C(54)-C(49)-C(47)	123.4(4)
C(49)-C(50)-C(51)	121.0(5)
C(50)-C(51)-C(52)	119.1(5)
C(53)-C(52)-C(51)	121.2(5)
C(52)-C(53)-C(54)	120.2(6)
C(53)-C(54)-C(49)	121.3(5)
C(56)-C(55)-C(60)	117.9(4)
C(56)-C(55)-C(48)	122.3(4)
C(60)-C(55)-C(48)	119.8(4)
C(57)-C(56)-C(55)	121.8(5)
C(58)-C(57)-C(56)	119.4(6)
C(57)-C(58)-C(59)	121.1(5)
C(58)-C(59)-C(60)	119.8(5)
C(55)-C(60)-C(59)	120.0(5)
C(62)-C(61)-C(66)	118.4(4)
C(62)-C(61)-C(48)	118.3(4)
C(66)-C(61)-C(48)	123.3(4)
C(61)-C(62)-C(63)	120.3(6)
C(64)-C(63)-C(62)	118.8(6)
C(65)-C(64)-C(63)	121.1(6)
C(64)-C(65)-C(66)	120.3(6)
C(65)-C(66)-C(61)	121.1(5)